JOURNAL OF MATERIALS SCIENCE 27 (1992) 5547–5552

Micromechanism of a deformation process before crazing in a polymer during tensile testing

H. KAWABE, Y. NATSUME
Nippondenso Co. Ltd, 1-1 Showa-cho, Kariya 448, Japan
Y. HIGO, S. NUNOMURA
Precision and Intelligence Laboratory, Tokyo Institute of Technology, 4259 Nagatsuta Midori-ku, Yokohama 227, Japan

Polymers are popularly used for housing and parts of machines and equipment. However, their mechanical properties, especially the deformation process, have not been clarified. During tensile testing, crazes are thought to be a source of microcracking and fracture, but the relation between the craze formation process and the deformation process before crazing is not understood. In the present work, scanning acoustic microscopy and X-ray diffraction were used to investigate the micromechanism before craze formation in polymethylmethacrylate (PMMA) and polycarbonate (PC). The velocity change of the surface acoustic wave and X-ray diffraction intensity indicated that molecular orientation occurred in a very small area from early stages of plastic deformation. From the results it was thought that texture was heterogeneous and anisotropic in a very small area, the shape of the area was spheroidal with a longer radius in the direction perpendicular to the applied stress, and the molecular chain in the area was oriented parallel to the stress axis. The area is thought to increase with increasing plastic strain.

1. Introduction

Although polymers are commonly used for housing or parts of machines and equipment, they have not been used for parts requiring reliability, because their mechanical properties, especially the deformation process, are not well understood.

When the fracture process of a polymer during tensile testing is considered, crazes are thought to be a source of microcracks and fracture [1–3]. The crazes are easy to detect optically. However, the micromechanism of the deformation process before crazing is not understood, because of the difficulty of detection and observation.

It is thought that acoustic properties, which are reflected in the elastic modulus, defect size, density, molecular orientation, etc., should vary in the heterogeneous area according to the stress or strain present. Therefore, scanning acoustic microscopy provides quantitative information of the acoustic properties nondestructively and without contact with the material [4, 5].

In the present study, polymers of polymethylmethacrylate (PMMA) and polycarbonate (PC) were tested to investigate the micromechanism of deformation, with the purpose of clarifying the micromechanism before crazing during tensile test deformation by scanning acoustic microscopy (SAM) and X-ray diffraction (XRD) on PMMA and PC.

2. Experimental procedure

2.1. Materials and tensile specimens

Commercially available PMMA (80N) and PC (S2000) were used in this study. Both materials are thermoplastic and amorphous polymers. The mechanical properties of the materials used in this study are given in Table I, and Fig. 1 shows the dimensions of the specimen used. Specimens were prepared by injection moulding to obtain a surface smooth enough for SAM observation.

TABLE I Mechanical properties of the polymers tested

	PMMA	PC
Specific gravity	1.19	1.20
Tensile strength (MPa)	72.0	60.0
Modulus of elasticity (GPa)	3.4	2.3
Deflection temperature (°C)	89	145

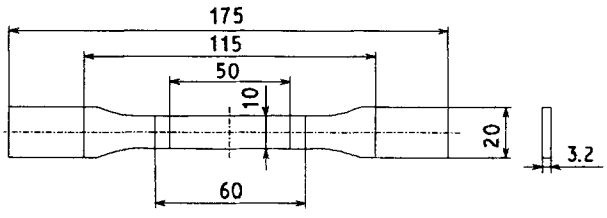

Figure 1 Shapes and dimensions (mm) of test specimens.

0022–2461

2.2. Tensile testing

Tensile tests were performed using a closed loop servohydraulic tensile test machine, under a strain rate of $3 \times 10^{-4}\ s^{-1}$, at 25 °C and a relative humidity of 55% (RH). The elongation of the specimen was measured during tensile testing by a clip gauge attached to the gauge length part of the specimen. The specimen was deformed until some pre-set strain, then unloaded for SAM observation and XRD measurement.

2.3. SAM observation and XRD measurement

Measurement of the surface acoustic wave (SAW) velocity by SAM (HSAM-1000S Hitachi) was performed on two kinds of specimen, pre-strained and virgin. On SAM, it has been found that the output of a piezoelectric transducer varied markedly with distance between the acoustic probe and the specimens [6, 7]. The relation between this output and the distance was called the $V(z)$ curve. It has been pointed out that a reflection acoustic microscope enables acoustic properties to be determined in solid materials. The characteristics of the periodicity of the dips on the $V(z)$ curve have been reported [8]. The results of measuring the dip interval depended on the material; it was uniquely and strongly related to the characteristics of solid materials. The dip interval is also closely related to the Rayleigh surface wave velocity on the specimen surface. Furthermore, by using a convergent anisotropy acoustic lens, the system can be applied for detecting the acoustic properties that reflect crystallographic anisotropies [5, 9].

In this experiment, the propagating velocity of SAW in the direction perpendicular or parallel to the applied stress on the surface, was measured using a convergent anisotropy acoustic lens. For the virgin specimen, the propagating velocity of SAW on the surface was measured using a point focus acoustic lens. The measured velocity was, therefore, an average value of all directions around the beam axis. All measurements were performed at a frequency of 400 MHz, and carried out at the centre of the specimen gauge length by scanning a 4.0 mm × 4.8 mm area. We determined the velocity of SAW by analysing the dip interval of the $V(z)$ curve. For several kinds of polymer, the mode of SAW has been reported to be the leaky surface skimming compressional wave (LSSCW) mode, and the velocity of the LSSCW was close to the longitudinal wave velocity along the plate [10, 11]. We describe the LSSCW velocity as the wave velocity in this paper. The temperature of pure water, used as the coupling medium between the acoustic lens and the specimen, was also measured for carbrating the measured velocity.

In order to measure the orientation in PC structure, XRD (RAD-RC Rigaku) was employed [12]. The measurement conditions are shown in Table II.

TABLE II XRD conditions

Characteristic X-ray	CuK_α
Tube voltage	50 kV
Tube current	300 mA
Scanning speed	$2° min^{-1}$
Irradiated area	2 mm diameter

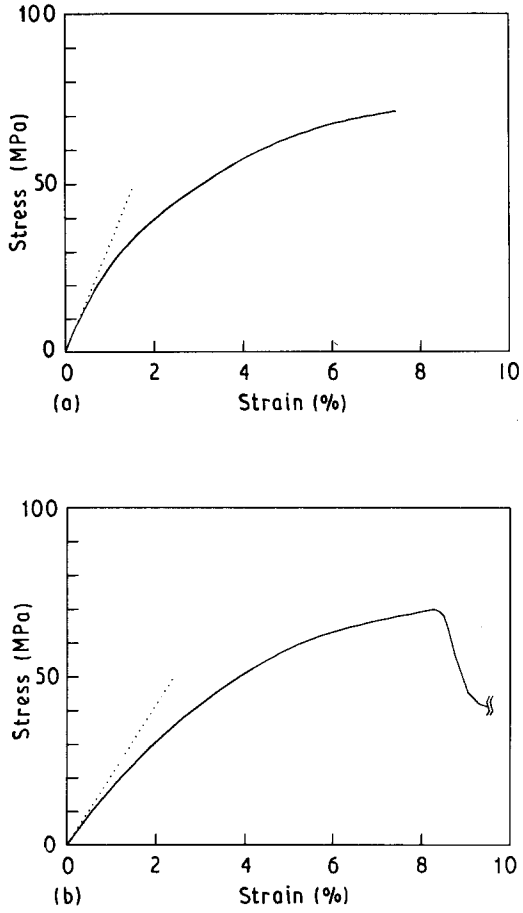

Figure 2 Stress–strain curves of (a) PMMA and (b) PC. (. . .)Elastic deformation obtained by elastic modulus.

3. Results

3.1. Tensile testing

Stress–strain curves of PMMA and PC are shown in Fig. 2. The stress increased gradually with increasing strain in both materials, as shown in Fig. 2. The boundary between the elastic and plastic deformation area is not clear. Dotted lines are the elastic deformation lines obtained from the elastic modulus. Therefore, the results suggest that both materials show only a little elastic deformation.

The difference in stress–strain curve characteristics of PMMA and PC is that the PMMA specimen indicated brittle failure, but the PC specimen indicated ductile failure after initiation of necking. The PC specimens for SAM observation were loaded under a strain below 8%, which corresponded to the initiation of necking.

After tensile testing, the surface behaviour of the pre-strained specimen was observed by optical microscopy. Fig. 3 shows PMMA (plastic strain 2.4%), and Fig. 4 shows PC (plastic strain 2.8%). Stress was applied in the allowed direction. In both figures, many crazes ran in a direction perpendicular to the applied stress. In PC, some crazes had shear bands at their ends.

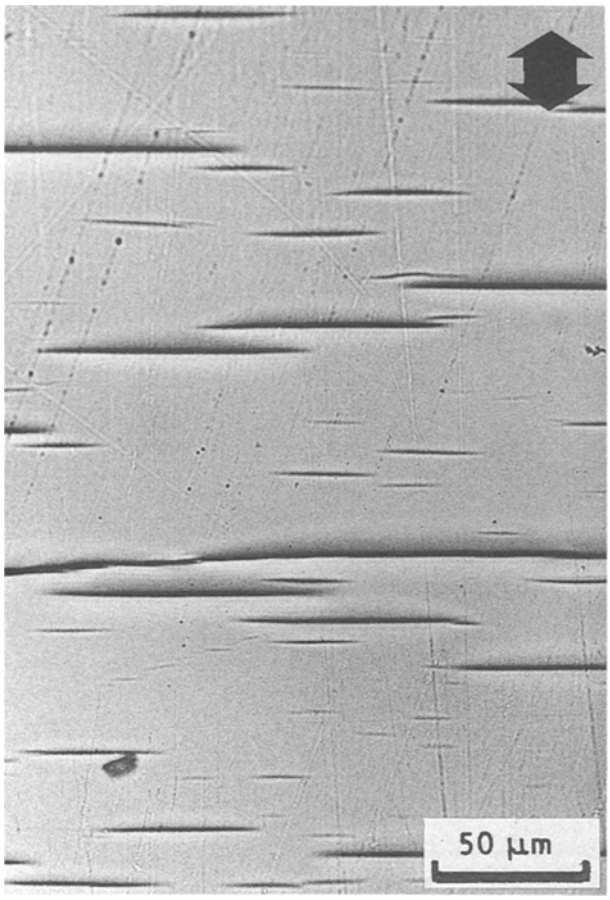

Figure 3 Optical micrograph of PMMA after applying 2.4% plastic strain. The loading direction is indicated by the arrow.

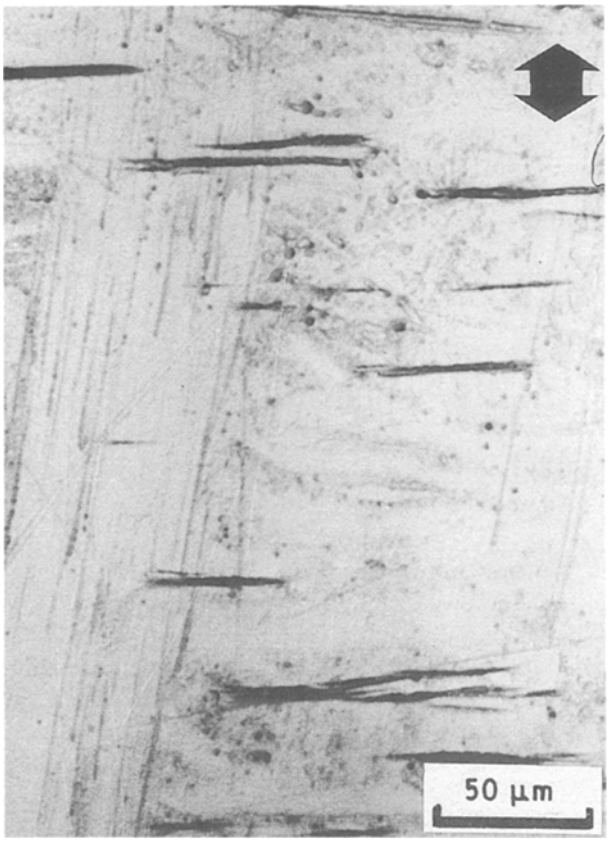

Figure 4 Optical micrograph of PC after applying 2.8% plastic strain. The loading direction is indicated by the arrow.

3.2. SAM observation and XRD measurement

The distribution of reflected signal intensity obtained in the X–Z mode by SAM on virgin specimens of PMMA and PC is shown in Fig. 5. The vertical direction indicates the direction of specimen depth, the horizontal direction indicates the direction along the specimen width. In the figures, the brightest horizontal line corresponds to the reflected signal from the specimen surface. Fig. 5 shows the periodicity of the signal intensity along the vertical direction. Therefore, texture was thought to be homogeneous for both specimens. From the distribution results, $V(z)$ curves were obtained and wave velocity was determined from the dip intervals of the $V(z)$ curves.

Wave-velocity measurement by SAM was performed in pure water. Therefore, the effect of water absorption on wave velocity should be clarified.

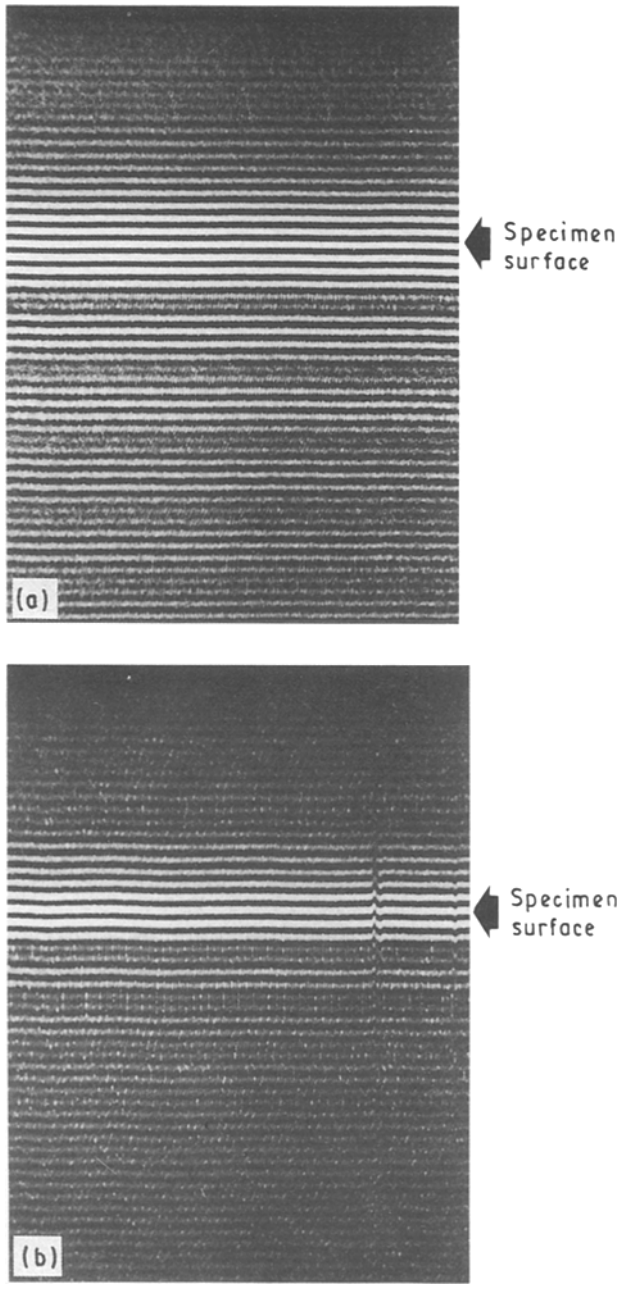

Figure 5 Typical results of x–z mode in PMMA and PC. The vertical direction indicates specimen depth; the horizontal direction indicates specimen width. The brightest horizontal line corresponds to the reflected signal from the specimen surface.

Wave-velocity change was measured during absorption in pure water. Fig. 6 shows relation between wave velocity and time in water. The effect of water absorption is negligibly small for the materials up to 10 h immersion in pure water. Therefore, the measurement of wave velocity was performed within this time. However, over 1000 h in water, the wave velocity changed considerably in both materials [13].

The relation between wave-velocity change and plastic strain found by using a convergent anisotropy acoustic lens is shown in Fig. 7a for PMMA, and Fig. 7b for PC. The vertical axis indicates wave-velocity change normalized by the wave velocity on the virgin specimen. The wave-velocity change of SAW in a direction perpendicular or parallel to the applied stress is shown. The horizontal axis indicates plastic strain. The results of wave velocity on virgin specimens measured using a convergent anisotropy acoustic lens and a point focus acoustic lens is shown in Table III. In Fig. 7a, the wave velocity in the direction perpendicular to the applied stress decreased linearly with increasing plastic strain. However, the wave velocity in the parallel direction hardly decreased. Therefore, the texture indicated anisotropies. On the other hand, the wave velocity in the direction perpendicular or parallel to the applied stress had the same value. Further, the wave-velocity results measured by a line focus lens and a point focus lens were almost the same as in Table III. Therefore, the texture was isotropic on virgin specimens. The sense of the results was the same in both PMMA and PC.

XRD measurements of PC revealed the relation between plastic strain and diffraction intensity around a diffraction angle at $2\theta = 17°$. The diffraction profile

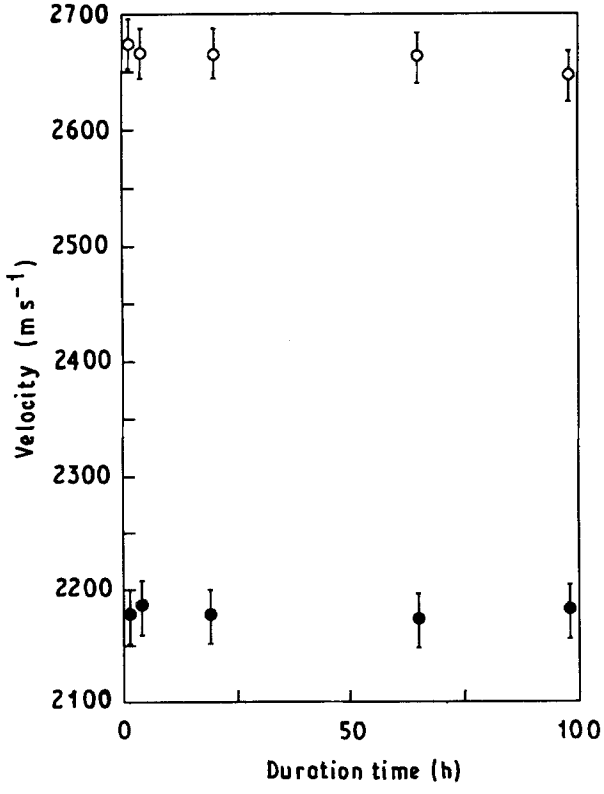

Figure 6 Relation between LSSCW velocity and time in water. (○) PMMA, (●) PC.

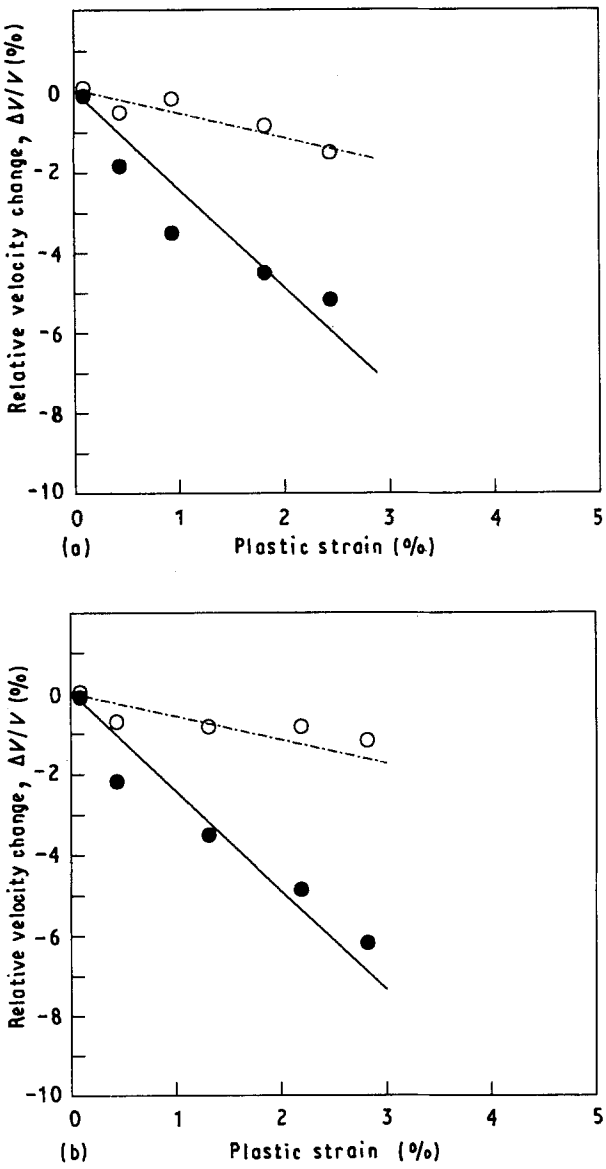

Figure 7 Relation between relative velocity change and plastic strain for (a) PMMA and (b) PC, (○) perpendicular and (●) parallel to the applied strain.

TABLE III LSSCW velocity on virgin specimens of PMMA and PC

Direction	Velocity (m s^{-1})	
	PMMA	PC
Perpendicular	2674	2197
Parallel	2702	2217
Point focus	2643	2179

in the direction perpendicular or parallel to the applied stress was measured. Fig. 8 shows a typical example of a diffraction profile obtained under 2.8% plastic strain. A diffraction peak was observed at the diffraction angle of 17°. Fig. 9 shows the relation between plastic strain and relative intensity change in the direction perpendicular or parallel to the applied stress. The relative intensity change, K, was used to avoid the effect of specimen thickness, and the relation may be represented by

$$K = PE/PA \quad (1)$$

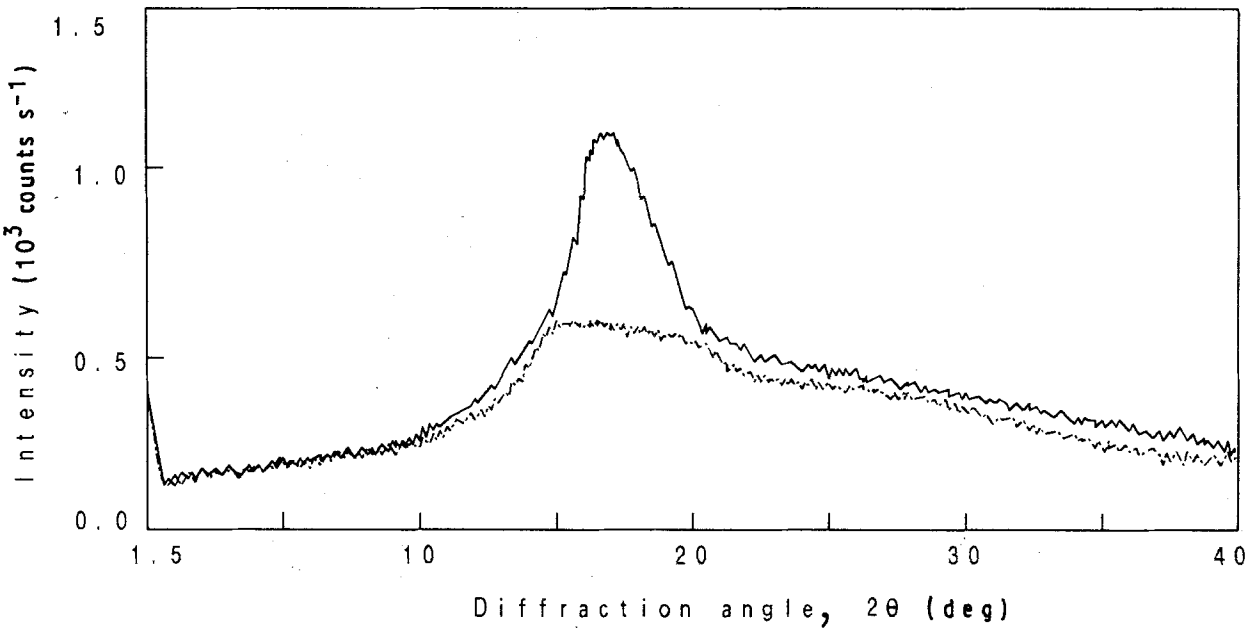

Figure 8 Typical example of the diffraction profile in PC (——) perpendicular and (·–·–) parallel to applied strain. The plastic strain was 2.8%, and diffraction peak angle was 17°.

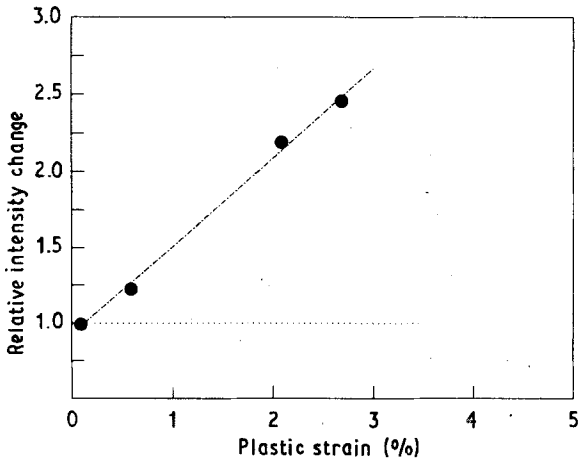

Figure 9 Relative intensity change of the diffraction profile versus plastic strain in PC.

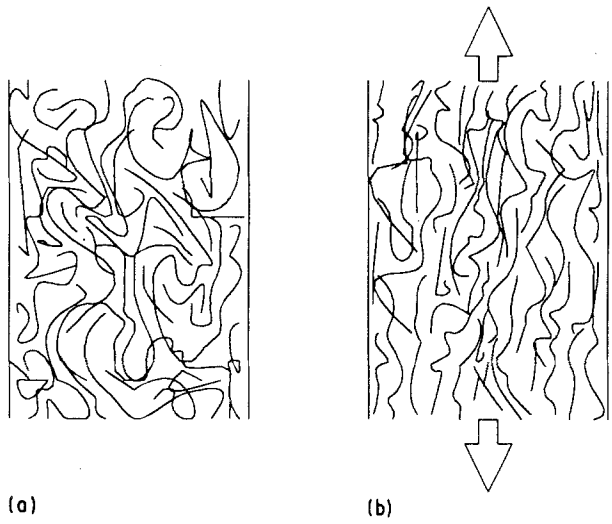

Figure 10 Schematic figures showing the micromechanism of the deformation process before crazing, assuming the texture is homogeneous and anisotropic. (a) undeformed, (b) deformed.

where PE and PA are diffraction intensity in the direction perpendicular and parallel to the applied stress, respectively. The vertical axis indicates the change in K, the horizontal axis indicates plastic strain. With increasing plastic strain, the relative intensity change, K, increased linearly.

4. Discussion

It is known that the micromechanism of deformation before crazing in amorphous polymer during tensile testing is as follows. Molecular chains are not oriented on virgin specimens, as shown schematically in Fig. 10a. Therefore, the texture is thought to be homogeneous and isotropic. If we assume in the micromechanism that texture is anisotropic and homogeneous, as shown in Fig. 10b, molecular chains should orient gradually with increasing stress.

According to the XRD results, the diffraction intensity in the direction perpendicular or parallel to the stress applied was almost the same on virgin specimens. With increasing plastic strain, the relative intensity change increased linearly. In Fig. 9, the results suggest that some molecular chains are oriented linearly to the plastic strain in the direction parallel to the applied stress. Here, we should note that the diffraction intensity is influenced by orientation and crystallization. PC is an amorphous polymer, and thermal hysteresis was not applied in this study. Therefore, it is considered that the diffraction intensity is almost dependent on the orientation of the molecular chain. Therefore, the results of XRD measurement agree well with the assumption of Fig. 10.

On the other hand, from the results of wave-velocity measurement by SAM, the wave velocity in a direction parallel to the applied stress decreased with increasing plastic strain. The velocity in the perpendicular direction decreased only slightly compared to others. In general, the longitudinal wave velocity, V, along a plate is represented by

$$V = E/[\rho(1 - \nu)^2]^{1/2} \quad (2)$$

where E is the elastic modulus, ρ the density, ν is Poisson's ratio [14]. In order to decrease wave velocity in the direction parallel to the applied stress, the elastic modulus must decrease, or the density must increase, from Equation 2. However, the elastic modulus in the parallel direction ought to increase because of the oriented molecular structure. If the density increases, the wave velocity should decrease in both directions. Therefore, the results of wave-velocity measurement are in contradiction with the assumption of Fig. 10.

Now, we propose another assumption in the micromechanism that the molecular chains will orient heterogeneously as schematically shown in Fig. 11a. It is considered that an oriented fibril structure, which is very similar to that in a craze, is constructed in a very small area compared to the craze. This is thought to be the embryo of crazing. In this area, the elastic modulus will increase and the density decreases because of the fibril structure. Thus acoustic velocity will be very different from a non-oriented area. Therefore, acoustic impedance becomes very high, and SAW should be scattered or diffracted at a locally oriented area, and SAW will propagate by a roundabout path through the locally oriented area. Wave velocity should decrease because the propagation path of SAW increases. However, these characteristics alone could not explain the anisotropies of SAW velocity.

We now consider the shape of a locally oriented area, for example, the embryo of crazing. Assuming that the shape is spherical, the results of wave velocity should be isotropic. Therefore, the shape is thought to be spheroid with a longer radius in the direction perpendicular to the applied stress, similar to the craze shown in Fig. 11b. In this case, the propagating path of SAW in the direction parallel to the applied stress should increase, because SAW will propagate by a roundabout path through the embryo of crazing. On the other hand, the propagation path in the perpendicular direction should increase slightly.

Referring to Fig. 7, the anisotropies of SAW velocity were observed from early stages of plastic deformation. Therefore, embryo crazing is produced when plastic deformation occurs, and the area develops further with increasing plastic strain. Finally, it may be observed optically as a craze.

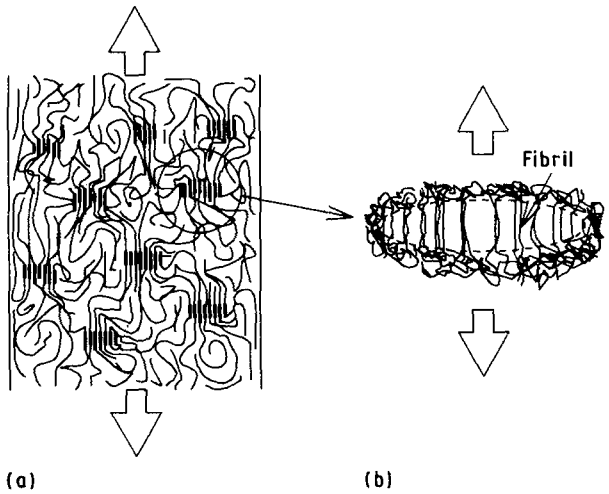

Figure 11 Craze embryo model of plastic deformation. (b) Magnification of (a).

5. Conclusions

The micromechanism of the deformation process before crazing has been described using SAM and XRD. Amorphous polymers PMMA and PC were used. Material characterization was made by quantitatively determining SAW velocity and XRD diffraction intensity. The following conclusions were drawn.

1. From the results of the SAW velocity measurement by SAM, the propagating velocity of the SAW in the direction parallel to the applied stress decreased, but the velocity in the perpendicular direction decreased only slightly. Thus the acoustic property indicated anisotropies.
2. From the XRD results, the relative intensity change was found to increase linearly with increasing plastic strain. The results suggested that some molecular chains were oriented in a direction parallel to the applied stress.
3. The micromechanism of the deformation process before crazing is as follows. Molecular chains locally were oriented in a very small area with increasing stress. Therefore, the texture became heterogeneous and anisotropic. It is considered that a fibril structure is constructed in the locally oriented area, which are thought to be embryo crazing.
4. The shape of the embryo crazing is spheroid with a longer radius in the direction perpendicular to the applied stress. The molecular chains of this area were oriented parallel to the stress axis.
5. The embryo crazing was produced from the early stages of plastic deformation, and developed with increasing plastic strain.

References

1. M. E. MACKAY and T. G. TENG, *J. Mater. Sci.* **14** (1979) 221.
2. C. CLAIBORNE and B. CRIST, *Colloid Polym. Sci.* **257** (1979) 457.
3. T. TAKEMURA and S. SHICHIJYO, *J. Soc. Rheol. Jpn* **13** (1985) 70.
4. I. ISHIKAWA, Scanning acoustic microscope technical paper, The Institute of Electronics, Information and Communication Engineers (1989) pp. 59–76.
5. I. ISHIKAWA and T. SENBA, Proceedings of the Spring Conference, Jpn Soc. Precision Engng (1990) p. 1111.
6. W. PARMAN and H. L. BERTONI, *Electron Lett.* **15** (1979) 684.
7. A. ATALAR, *J. Appl. Phys.* **50** (1979) 8237.
8. R. D. WEGLEIN, *Appl. Phys. Lett.* **34** (1979) 179.
9. I. ISHIKAWA and Y. KONOMURA, *IEEE*, to be published.
10. J. KUSHIBIKI, *IEEE Trans. Sonics Ultrasonics* **SU-32** (2) (1985) 189.
11. K. YAMANAKA, Scanning acoustic microscope technical paper, The Institute of Electronics, Information and Communication Engineers (1989) pp. 17–31.
12. M. KAKUDO and C. KASAI, "X-ray diffraction in polymer" (Maruzen, 1968) pp. 262–82.
13. H. KAWABE, *JSME*, to be published.
14. "Ultrasonic Technology Manual" (The Nikkan Kogyo Shimbun Ltd) 1978.

Received 26 June
and accepted 28 November 1991